CUTTING FORCE MODELLING WITH EFFECTS OF CUTTING TOOL GEOMETRY AND TOOL WEAR IN MILLING OF DIN C45 STEEL

JAROSLAV KOVALCIK[12], PAVEL ZEMAN[1], FRANTISEK HOLESOVSKY[2], JAN MADL[2], LUDMILA KUCEROVA[3]

[1]Department of Production Machines and Equipment, Faculty of Mechanical Engineering, Czech Technical University in Prague, Czech Republic

[2]Department of Machining, Process Planning and Metrology, Faculty of Mechanical Engineering, Czech Technical University in Prague, Czech Republic

[3]Department of Material Science and Technology, Faculty of Mechanical Engineering, University of West Bohemia, Pilsen, Czech Republic

DOI: 10.17973/MMSJ.2020_03_2019124

e-mail: j.kovalcik@rcmt.cvut.cz

This paper focuses on mathematical modelling of cutting force with tool wear effect for milling by milling heads. With regard to a small number of experiments with sufficient accuracy, universality, speed and applicability in practice, a mathematical model based on the specific cutting force and cutting area was created. The proposed mathematical model is more refined than other models owing to more accurate calculation of the specific cutting force and cutting area. The calculation of the specific cutting force is more precise due to consideration of the influence of the cutting speed, more accurate calculation of the undeformed chip thickness and implementation of the correction factor of the tool flank wear, which has a significant impact on the cutting force. The calculation of the cutting area is achieved through more accurate calculation of the chip width as well as undeformed chip thickness. The chip width and undeformed chip thickness are refined by consideration of the straight and rounded parts of the cutting edge. For the proposed mathematical model, material constants for the workpiece material made of DIN C45 steel were obtained.

KEYWORDS

Milling, cutting force, specific cutting force, tool wear, C45 steel

1 INTRODUCTION

This article is a follow-up to the previous article which is listed in the references [Kovalcik 2014]. In that article, some basic techniques and approaches to cutting process modelling were introduced along with their advantages and disadvantages. These methods include:

- FEM modelling and material modelling, see references [Katsuhiro 2005, Roud 2011, Zeman 2005],
- prediction using an artificial neural network, see references [Dobrzanski 2005, Irgolic 2013, Mavi 2016],
- modeling based on empirical equations, see references [Constantin 2013, Starchurski 2012, Zhang 2018],
- modelling based on specific cutting force and cutting area, which are categorized by force model type:
  - linear model, see references [Aksu 2016, Altintas 2012, Vasilko 2007, Vavruska 2018],
  - power model, see references [Degner 2015, Horvath 2017, Tschatsch 2009, Velchev 2011].

Based on the review, we found that all of the modelling methods contain some limitations and/or simplifications. This fact leads to quite different results in terms of outputs, accuracy, calculation speed, universality and applicability in practice. The most suitable modelling method for the calculation of the cutting force, in my opinion, is a method based on the product of the specific cutting force (k_c) and cutting area (A_D), where the basic form of the specific cutting force is based on the impact of the undeformed chip thickness (h_D); see equation (1).

$$\left.\begin{aligned} k_c &= k_{c_{1.1}} \cdot h_D^{-m_c} \\ A_D &= h_D \cdot b_D \end{aligned}\right\} F_c = k_c \cdot A_D = k_{c_{1.1}} \cdot h_D^{1-m_c} \cdot b_D \qquad (1)$$

This method is applicable to machining technologies with tools that have a defined cutting edge geometry, i.e. milling, turning, drilling and boring. In practice, this methodology is used by the world's leading cutting tool manufacturers in their software applications. These applications are based on mathematical models, which are, however, very simplified, and so significant errors occur during cutting force prediction. In order to predict more precise values of force effects during milling, a more sophisticated mathematical model is needed.

2 PROPOSED CUTTING FORCE MATHEMATICAL MODEL

The basic form of equation (1) can be refined by more accurate calculation of the cutting area (A_D) and the specific cutting force (k_c). We increase the accuracy of the calculation of the cutting area by making the undeformed chip thickness (h_D) and chip width (b_D) more precise by considering the straight as well as the rounded part of the cutting edge. The specific cutting force calculation will be made more accurate by considering the influence of the cutting speed on the specific cutting force and also by making the afore mentioned undeformed chip thickness more precise.

The proposed mathematical model will be applicable to cutting tool inserts of both circular and non-circular cross-sections (square, triangular cross-section). If a cutting tool insert has a circular cross-section, the mathematical model will work with the R value equal to half of the diameter of the cutting tool insert ($D_d/2$). If a cutting tool insert has a non-circular cross-section, the mathematical model will work with the R value equal to the corner radius (r_ε).

2.1 Calculation of the chip width and actual value of the undeformed chip thickness

To calculate the actual and mean cutting force values, it is necessary to propose equations for the chip width and the actual value of the undeformed chip thickness, when acting on the rounded as well as the straight part of the cutting edge. The calculation of the actual value of the undeformed chip thickness is based on the division of the actual value of the cutting area and chip width; see equation (2).

$$h_D(\varphi) = A_D(\varphi)/b_D \qquad (2)$$

The first step is to calculate the actual value of the cutting area. In order to do that, the cutting area in a given engagement angle was divided into two areas – the area where only the straight part of the cutting edge acts, i.e. $A_{D1}(\varphi)$, and the area where only the rounded part of the cutting edge acts, i.e. $A_{D2}(\varphi)$; see Figure 1. The actual value of the cutting area is then given by the sum of the two areas; see equation (3).

$$A_D(\varphi) = A_{D_1}(\varphi) + A_{D_2}(\varphi) \qquad (3)$$

The chip width is calculated based on the sum of the chip width of the straight and rounded parts; see equation (4).

$$b_D(\varphi) = b_{D_1}(\varphi) + b_{D_2}(\varphi) \quad (4)$$

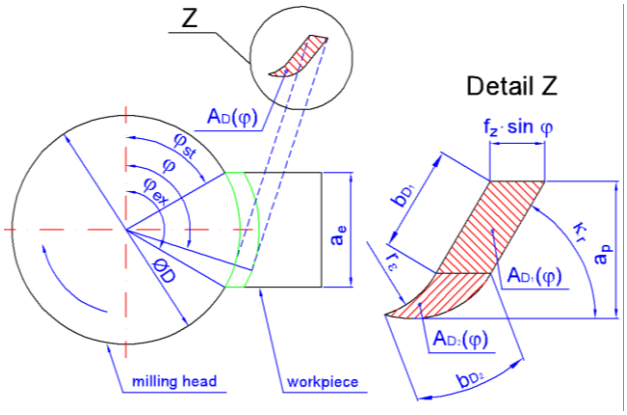

Figure 1. Cutting area for a given actual engagement angle

Straight part of the cutting edge

The axial depth of cut can be set so that it is machined either by only the rounded part of the cutting edge or the rounded as well as the straight part of the cutting edge. If the condition $a_p \le R \cdot (1 - \cos\kappa_r)$ is met, it is machined only by the rounded part of the cutting edge. In this case, the undeformed chip thickness, chip width as well as the cutting area of the straight part of the cutting edge are equal to 0. If the previously mentioned condition is not met, it is machined by the rounded as well as the straight part of the cutting edge. For this case, we have to define the equations for calculating the undeformed chip thickness, chip width and cutting area of the straight part of the cutting edge.

According to Figure 1, the actual value of the undeformed chip thickness of the straight part of the cutting edge is calculated based on equation (5). The chip width of the straight part of the cutting edge is calculated by equation (6). Based on equations (5) and (6), the equation for the actual cutting area of the straight part of the cutting edge is obtained; see equation (7).

$$h_{D_1}(\varphi) = f_z \cdot \sin\varphi \cdot \sin\kappa_r \quad (5)$$

$$b_{D_1} = \frac{a_p - R \cdot (1 - \cos\kappa_r)}{\sin\kappa_r} \quad (6)$$

$$A_{D_1}(\varphi) = h_{D_1}(\varphi) \cdot b_{D_1} = f_z \cdot \sin\varphi \cdot \left[a_p - R \cdot (1 - \cos\kappa_r)\right] \quad (7)$$

Rounded part of the cutting edge

The rounded part of the cutting edge always cuts the workpiece material differently than the straight part. According to Figure 1, the actual undeformed chip thickness of the rounded part of the cutting edge is calculated based on equation (8). The element of the chip width of the rounded part of the cutting edge is calculated based on the radius (R) and the element of the acting angle of the rounded part of the cutting edge (θ); see equation (9). Based on equations (8) and (9), the equation for the actual value of the element of the cutting area of the rounded part of the cutting edge is obtained; see equation (10).

$$h_{D_2}(\varphi, \theta) = f_z \cdot \sin\varphi \cdot \sin\theta \quad (8)$$

$$db_{D_2} = R\, d\theta \quad (9)$$

$$dA_{D_2}(\varphi, \theta) = h_{D_2}(\varphi, \theta) \cdot db_{D_2} = f_z \cdot \sin\varphi \cdot R \cdot \sin\theta\, d\theta \quad (10)$$

After the integration of equations (9) and (10) within the starting (θ_{st}) and ending (θ_{end}) angles of acting the rounded part of the cutting edge, the equations for the chip width and actual value of the rounded part of the cutting edge are obtained; see equations (11) and (12).

$$b_{D_2} = R \cdot (\theta_{end} - \theta_{st}) \quad (11)$$

$$A_{D_2}(\varphi) = f_z \cdot \sin\varphi \cdot R \cdot (\cos\theta_{st} - \cos\theta_{end}) \quad (12)$$

The starting angle of the action of the rounded part of the cutting edge (θ_{st}) is calculated by equation (13). The ending angle of the action of the rounded part of the cutting edge (θ_{end}) is calculated based on the condition of whether only the rounded part of the cutting edge cuts the workpiece material, or both the straight and the rounded parts cut the workpiece; see equation (14).

$$\theta_{st} = -\arcsin\frac{f_z}{2 \cdot R} \quad (13)$$

$$\theta_{end} = \begin{cases} \kappa_r & a_p > R \cdot (1 - \cos\kappa_r) \\ \arccos\dfrac{R - a_p}{R} & a_p \le R \cdot (1 - \cos\kappa_r) \end{cases} \quad (14)$$

2.2 *Calculation of the actual value of the cutting force*

The calculation of the actual value of the cutting force is important for plotting the cutting force over time in a certain interval, as well as for the calculation of the mean value of the cutting force, since the mean value is based on the integration of the function of the actual cutting force within the starting and ending engagement angles. The actual values of the cutting force in one revolution for full immersion milling (a_e=D) with three teeth in engagement are plotted on Figure 2.

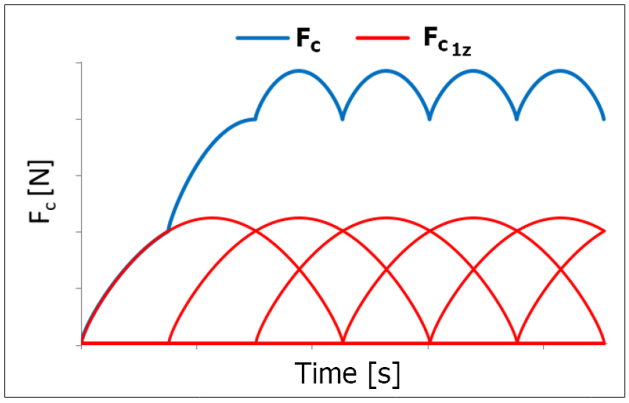

Figure 2. Actual values of the cutting force in one revolution for full immersion milling with three teeth in engagement: total cutting force (blue curve), cutting force per 1 tooth (red curve).

The value of the total cutting force at each engagement angle $F_c(\varphi)$ is given by the sum of the cutting forces acting on the individual teeth of the cutting tool; see equation (15).

$$F_c(\varphi) = \sum_{i=1}^{Z_e} F_{c_{1z}}(\varphi_i(\varphi)) \quad (15)$$

The value of the cutting force per tooth at each engagement angle is calculated based on the product of the actual value of the specific cutting force and cutting area, where the cutting area is the product of the undeformed chip thickness and chip width; see equation (16).

$$F_{c_{1z}}(\varphi_i(\varphi)) = k_c(\varphi_i(\varphi)) \cdot h_D(\varphi_i(\varphi)) \cdot b_D \quad (16)$$

The actual value of the specific cutting force is calculated based on equation (17), which includes the impact of the undeformed chip thickness (the basic form of the equation) as well as the impact of the cutting speed (the added part of the equation).

$$k_c(\varphi_i(\varphi)) = k_{c_{1.1}} \cdot h_D(\varphi_i(\varphi))^{-m_c} \cdot \left(\frac{v_c}{v_{c_{def}}}\right)^{-m_{v_c}} \quad (17)$$

The final equation for the calculation of the cutting force per tooth for a given engagement angle is calculated according to equation (18).

$$F_{c_{1z}}(\varphi_i(\varphi)) = k_{c_{1.1}} \cdot h_D(\varphi_i(\varphi))^{1-m_c} \cdot \left(\frac{v_c}{v_{c_{def}}}\right)^{-m_{v_c}} \cdot b_D \qquad (18)$$

The actual value of the engagement angle of the i-th tooth is calculated based on the rotation angle of the cutting tool (φ) and the angle between teeth (φ_z); see equations (19) and (20).

$$\varphi_i(\varphi) = \begin{cases} \varphi - \varphi_z \cdot (i-1) & \varphi_{st} \le \varphi_i(\varphi) \le \varphi_{end} \\ 0 & \text{otherwise} \end{cases} \qquad (19)$$

$$\varphi_z = \frac{2 \cdot \pi}{Z} \qquad (20)$$

2.3 Calculation of the mean value of the cutting force

To calculate the mean value of the cutting force for Z teeth in engagement per revolution, the mean cutting force per tooth must be calculated first. For this calculation we will work with the general formula for the mean value of the function; see equation (21) on the left [Kolar 2016, Kopacek 2004]. The mean value of the cutting force per tooth is calculated using the basic formula of the mean value of a function based on the integration of the actual cutting force function per tooth within the starting and ending engagement angles; see equation (21) on the right.

$$\bar{f} = \frac{1}{b-a}\int_a^b f(x)\,dx \rightarrow F_{c_{m_{1z}}} = \frac{1}{\varphi_{end}-\varphi_{st}}\int_{\varphi_{st}}^{\varphi_{end}} F_{c_{1z}}(\varphi)\,d\varphi \qquad (21)$$

The mean value of the cutting force per tooth mentioned above is shown in Figure 3 with the actual value of the cutting force per tooth.

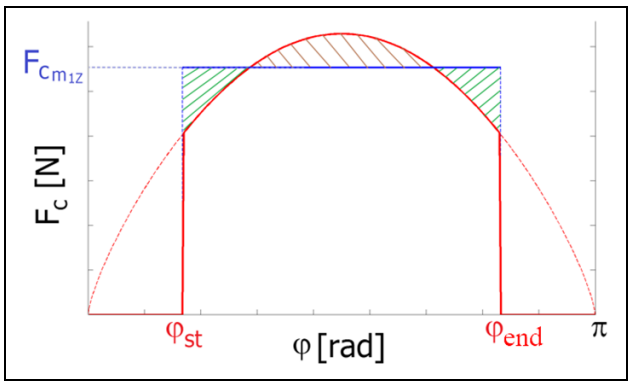

Figure 3. Actual value of the cutting force per tooth (bold red) and mean value of the cutting force per tooth (blue).

After the substition of the equation for the actual cutting force per tooth, the final form of the equation for the mean cutting force per tooth is obtained; see equation (22).

$$F_{c_{m_{1z}}} = \frac{1}{\varphi_{eng}} \cdot k_{c_{1.1}} \cdot \left(\frac{v_c}{v_{c_{def}}}\right)^{-m_{v_c}} \cdot b_D \cdot \int_{\varphi_{st}}^{\varphi_{end}} h_D(\varphi)^{1-m_c}\,d\varphi \qquad (22)$$

The integral in the previous equation has no simple analytical solution. The solution is to use software such as Matlab.

2.4 Starting and ending engagement angles

The starting (φ_{st}) and ending (φ_{end}) engagement angles depend on the milling strategy. There are 3 types of strategies for milling heads: full immersion, face milling and side milling (up-milling and down-milling). The equations for the calculation of the starting and ending engagement angles for these strategies are summarized in Table 1.

Milling strategy	Starting angle	Ending angle
Full immersion 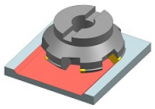	$\varphi_{st} = 0$	$\varphi_{end} = \pi$
Face milling 	$\varphi_{st} = \arccos\left(\frac{\frac{a_e}{2}+e}{\frac{D}{2}}\right)$	$\varphi_{end} = \pi - \arccos\left(\frac{\frac{a_e}{2}-e}{\frac{D}{2}}\right)$
Side down-milling 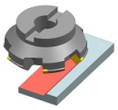	$\varphi_{st} = \arccos\left(\frac{\frac{a_e}{2}-e}{\frac{D}{2}}\right)$	$\varphi_{end} = \pi$
Side up-milling 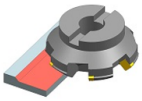	$\varphi_{st} = 0$	$\varphi_{end} = \pi - \arccos\left(\frac{a_e-\frac{D}{2}}{\frac{D}{2}}\right)$

Table 1. Equations for calculating the starting and ending engagement angles for different milling strategies.

3 OBTAINING MATERIAL CONSTANTS FOR THE PROPOSED MATHEMATICAL MODEL

In the previous chapter, a mathematical model for calculating the specific cutting force (k_c) with the influence of the cutting speed (v_c) was proposed. There are three constants in the equation that have to be determined for each workpiece material. The material constant $k_{c1.1}$ is a specific cutting force for a cutting area of 1 mm² (h=b=1mm) and for the default value of the cutting speed v_{cdef}. The cutting speed v_c is the cutting speed for which the specific cutting force is calculated. The material constant m_c determines the effect of the undeformed chip thickness (h_D) on the specific cutting force (k_c). The constant m_{vc} determines the influence of the cutting speed on the specific cutting force. To obtain these three constants, it is necessary to propose appropriate experiments.

3.1 Preparation of experiments

These experiments were performed on DIN C45 steel with a measured hardness of 200 HV 10. The chemical composition was measured using EDS analysis: 0.41% Si, 0.29% Cr, 0.8% Mn and 0.2 % Mo. The sulphur and phosphorus contents were below the detected values. It was not possible to determine the carbon content through EDS analysis.

A SECO R220.17-0125-22 cutting tool with a TPKN2204PPR-M14 uncoated cutting tool insert was used to determine the material constants; see Table 2.

Cutting tool	Designation	SECO R220.17-0125-2
	Cutting tool diameter (D)	125 mm
	Number of teeth (N)	6
	Lead angle (κ_r)	90°
	Inclination angle (λ_s)	0°
	Rake angle after inserting the CTI (γ_0)	0°
Cutting tool insert (CTI)	Designation	TPKN2204PPR-M14
	Coating	No coating
	Shape	Triangle
	Number of cutting edges	3
	Clearance angle (α_0)	11°
	Rake angle (γ_0)	0°

Table 2. Parameters of the SECO R220.17-0125-22 cutting tool

Table 3 shows the percentage composition of the core and surface elements of the TPKN2204PPR-M14 cutting tool insert.

Tungsten carbide (WC) [%]				Cobalt (Co) [%]	
Core		Surface		Core	Surface
W [%]	C [%]	W [%]	C [%]		
74.59	16.78	72.80	19.23	8.63	7.97
91.37		92.03			

Table 3. Percentage composition of the TPKN2204PPR-M14 insert.

Although the producer of this cutting tool insert does not recommend it for cutting steel workpieces, it was used for these reasons: zero rake angle, no chip breaker, no chamfer and cutting tool with zero inclination angle. This enabled material constants to be determined relatively accurately.

The experiments were carried out at the Research Institute of Textile Machinery in Liberec (VUTS Liberec), Czech Republic, on a WHN 13 CNC horizontal milling and boring machine made by the company TOS Varnsdorf, Czech Republic.

3.2 *Force measurement and cutting force evaluation*

A 9255B stationary piezoelectric dynamometer was used to measure forces (F_x, F_y, F_z) in milling; see Figure 4.

First of all, it was necessary to transfer the measured forces from the dynamometer coordinate system (the F_x, F_y forces) to the cutting tool coordinate system (the F_c force) at each engagement angle. In order to obtain the equation for the cutting force calculation we use Figure 4.

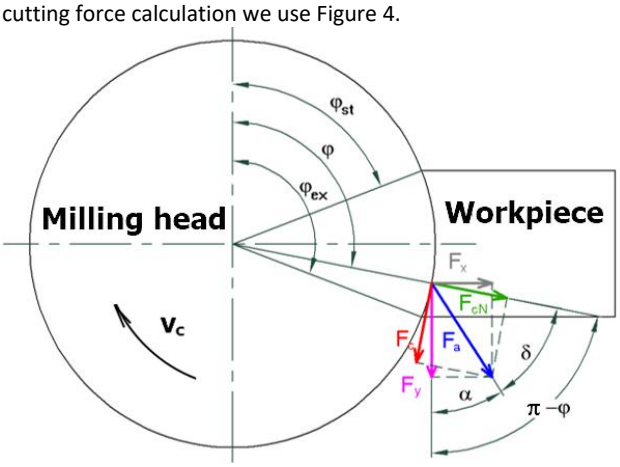

Figure 4. Force decomposition in face milling strategy by a milling head.

Based on Figure 4, the cutting force is calculated using equation (23). In this equation, there is the active force $F_a(\varphi)$ and the angle between the $F_a(\varphi)$ and $F_y(\varphi)$ forces, i.e. $\alpha(\varphi)$. These values are calculated using equations (24) and (25).

$$F_c(\varphi) = F_a(\varphi) \cdot \sin(\pi - \varphi - \alpha(\varphi)) \tag{23}$$

$$F_a(\varphi) = \sqrt{F_x^{\,2}(\varphi) + F_y^{\,2}(\varphi)} \tag{24}$$

$$\alpha(\varphi) = \operatorname{arctg}\frac{F_x(\varphi)}{F_y(\varphi)} \tag{25}$$

After we had the cutting force in time, the mean value of the cutting force per engagement in a selected interval was evaluated. For this purpose, a software application in Matlab was created. This software automatically found the starting and ending points of each engagement and the angle φ as interpolated within these engagement angles.

3.3 *Proposed measurement methodology*

In order to create a mathematical model that would be applicable to cutting tools with different geometries, more precisely, with different corner radiuses, we decided to cut the workpiece material without the effect of the corner radius. For this purpose, a sample with a fixture was designed; see Figure 5. The sample has a rectangular cross-section with dimensions of 100 x 45 mm (length x width) and various thicknesses (see Table 4, depth of cut values). For this sample, a fixture was proposed that would work well with the sample in every measurement, because after each measurement the sample had to be moved forward.

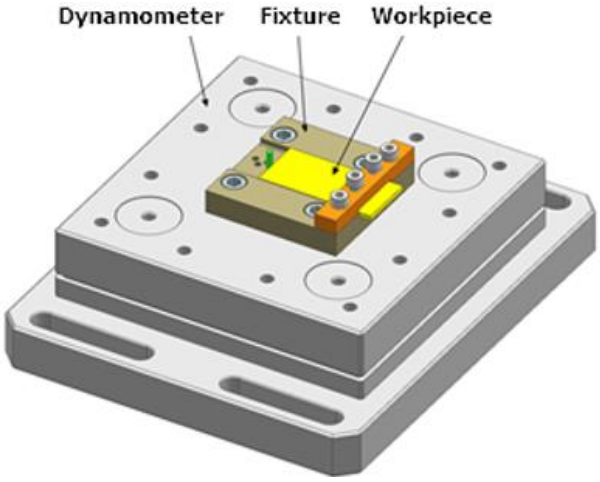

Figure 5. The proposed fixture with a workpiece placed on the KISTLER 9255b dynamometer.

3.4 *Design of experiments*

In order to design the experiments, central composite planning was used. Various software (Statistica, Design of experts, Minitab) enables this type of experiment planning. The general scheme of the composite experiment planning for three factors is shown in Figure 6a.

The total number of points is given by the equation $2^k+2\cdot k+m$, so for 3 factors, there are 14+m points, where m is the number of center points. The minimum number of center points is 0, so the minimum total number of points is 14. For these experiments, 4 center points were chosen, so the total number of points is 18, which means 18 experiments.

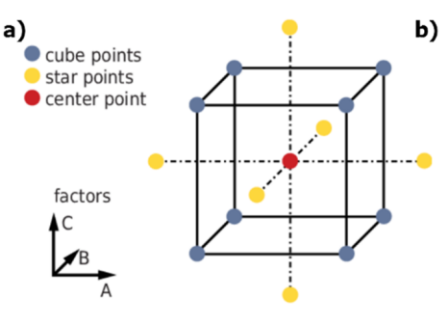

Type of points	Factors A	B	C
Cube points	-1	-1	-1
	+1	-1	-1
	-1	+1	-1
	-1	-1	+1
	+1	+1	-1
	+1	-1	+1
	-1	+1	+1
	+1	+1	+1
Star / axial points	−α	0	0
	+α	0	0
	0	−α	0
	0	+α	0
	0	0	−α
	0	0	+α
Center points	0	0	0
	0	0	0
	0	0	0
	0	0	0

Figure 6. a) General scheme of central composite planning of experiments for three factors; b) General proposal of experiments for three factors with three center points.

For experiment planning, the three factors (A, B, C) include the axial depth of cut (a_p), feed per tooth (f_z) and cutting speed (v_c). The general proposal of experiments for 3 factors with 4 center points is shown in Figure 6b.

The cutting conditions for the different levels of the central composite experiment plan are shown in Table 4, where α (see Figure 6b – star/axial points) is, for three factors and four center points, equal to 1.41421.

Parameter	-1.41421	-1	0	1	1.41421
a_p [mm]	4	4.3	5	5.7	6
f_z [mm]	0.090	0.109	0.155	0.201	0.220
v_c [m/min]	100	129	200	271	300

Table 4. Cutting conditions for different levels of the central composite experiment plan for milling of C45 steel.

3.5 *Evaluation of experiments*

Based on the methodology described in Chapter 3.2, the mean values of the cutting force from the measured force signals were evaluated. Each experiment was measured three times and from the three values, the mean value was obtained (F_c) with the standard deviation(s); see Table 5.

No.	a_p [mm]	f_z [mm]	v_c [m/min]	F_c [N]	s [N]
1	4.3	0.109	129	1223.5	10.55
2	5.7	0.109	129	1542.7	0.43
3	4.3	0.201	129	1810.2	3.17
4	4.3	0.109	271	1093.4	7.36
5	5.7	0.201	129	2345.9	0.28
6	5.7	0.109	271	1413.8	10.11
7	4.3	0.201	271	1563.4	2.34
8	5.7	0.201	271	2042.9	6.50
9	4	0.155	200	1388.6	3.58
10	6	0.155	200	1916.3	4.25
11	5	0.090	200	1182.4	2.22
12	5	0.220	200	2057.4	2.27
13	5	0.155	100	1879.4	10.07
14	5	0.155	300	1470.5	0.13
15	5	0.155	200	1583.0	5.55
16	5	0.155	200	1595.1	13.48
17	5	0.155	200	1598.6	12.43
18	5	0.155	200	1595.0	6.00

Table 5. Evaluation of the measured experiments.

The mean value of the standard deviation is 5.6 N with a range of 0.13 to 13.48 N. The highest standard deviation values were found at the midpoint (experiments 15 to 18) for experiments 16 and 17, for which the mean values of the cutting force were not very different from experiments 15 and 18, for which much smaller standard deviations were found. All mean values of cutting forces evaluated from experimental measurements were used to find material constants in Chapter 3.6.

3.6 *Obtaining material constants*

Principle of obtaining material constants

To obtain values of the specific cutting force, we should use the same equation that is used for the calculation of the cutting force, but in this case, the specific cutting force is not a function, but a constant that we want to get from each experiment; see equation (26).

$$F_{c_{m_{1z}}} = \frac{1}{\varphi_{eng}} \cdot k_c \cdot f_z \cdot a_p \cdot (\cos\varphi_{st} - \cos\varphi_{end}) \quad (26)$$

Based on the previous equation, the specific cutting force is calculated according to equation (27).

$$k_c = \frac{F_{c_{m_{1z}}} \cdot \varphi_{eng}}{f_z \cdot a_p \cdot (\cos\varphi_{st} - \cos\varphi_{end})} \quad (27)$$

As seen in the previous equation, the mean value of the undeformed chip thickness is given by equation (28).

$$h_{D_m} = f_z \cdot (\cos\varphi_{st} - \cos\varphi_{end}) \quad (28)$$

After the values of the specific cutting forces were calculated by equation (27), these values were entered as an output parameter into the Minitab software and the input parameters were: chip width (b_D), which is, in this case, equal to the axial depth of cut (a_p), the mean value of the undeformed chip thickness (h_{Dm}), as calculated by equation (28), and the cutting speed (v_c). In the Minitab software, a non-linear regression was selected with the equation of the specific cutting force with the influence of the cutting speed. All three material constants were thus determined.

Obtaining material constants for C45 steel

Based on this approach, by using the Minitab software, material constants were determined for C45 steel, so the mathematical model for the specific cutting force could be proposed; see equation (29).

$$k_c = k_{c_{1.1}} \cdot h_D^{-m_c} \left(\frac{v_c}{v_{c_{def}}} \right)^{-m_{v_c}} = 1048 \; h_D^{-0.38} \left(\frac{v_c}{200} \right)^{-0.179} \quad (29)$$

The value of the determination index (R^2) of the obtained mathematical model is 94.88% and the value of the adjusted determination index (R^2 Adj) is 94.19%.

Figure 7 shows the dependence of the calculated specific cutting force on the feed per tooth in the range of feeds per tooth from 0.09 to 0.22 mm for 5 values of the cutting speeds in the range from 100 to 300 m/min used for the experiments.

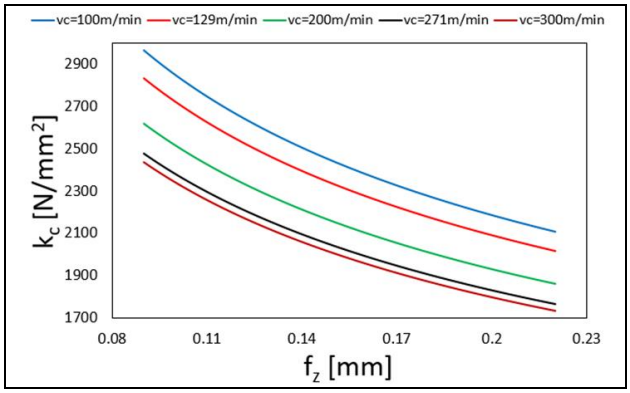

Figure 7. Dependence of the specific cutting force on the feed per tooth for five values of cutting speeds.

4 VERIFICATION OF THE PROPOSED MATHEMATICAL MODEL

In Chapter 2, a mathematical model was proposed which refines the calculation of the cutting force by more accurate calculation of the specific cutting force and cutting area. The calculation of the specific cutting force was refined by considering the influence of the cutting speed as well as by more precise calculation of the undeformed chip thickness. The calculation of the cutting area was refined by more accurate calculation of the chip width as well as the undeformed chip thickness. The chip width and undeformed chip thickness was made more precise by considering both the straight and rounded parts of the cutting edge. For the proposed model, material constants for C45 steel were obtained.

The next step was to verify the proposed mathematical model through suitable experiments to show the accuracy of the model.

4.1 *Preparation of experiments*

The same workpiece which had been used to obtain the material constants was used in this step.

The experiments were carried out using the SECO R220.17-0125-22 cutting tool, which is the same cutting tool which was used to obtain the material constants. The difference, however, is that these experiments were performed using the rounded as well as the straight part of the cutting edge. The technical parameters of the used cutting tool and cutting tool insert are summarized in Table 2.

The experiments were carried out at the Research Institute of Textile Machinery in Liberec (VUTS Liberec), Czech Republic, on a WHN 13 CNC horizontal milling and boring machine made by the company TOS Varnsdorf, Czech Republic.

4.2 Force measurement and cutting force evaluation

A stationary 9255B piezoelectric dynamometer was used to measure the forces F_x, F_y in milling; see Figure 4. The procedure to transfer these forces to the cutting force F_c is described in Chapter 3.2.

4.3 Measurement methodology proposal

In order to verify the mathematical model, experiments were carried out, in this case using a cutting tool with the influence of a rounded cutting edge. The workpiece was fixed on the dynamometer with two screws; see Figure 8.

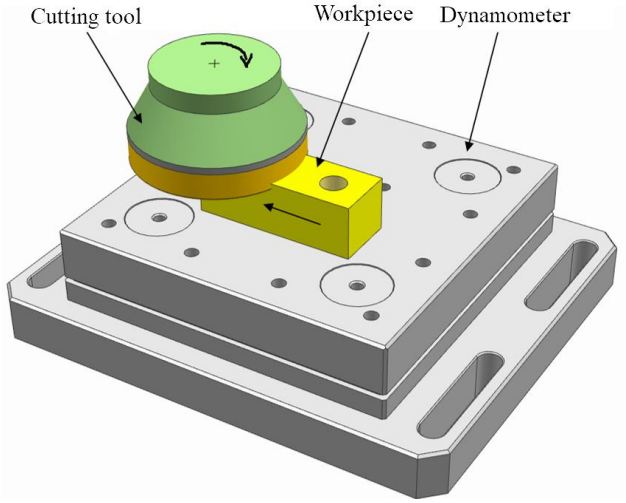

Figure 8. Workpiece placed on the Kistler 9255b dynamometer.

For these experiments, we used workpiece samples which were blocks of a rectangular cross-section of different widths (sample size - length x width x height: 120x25x40, 120x35x40 and 120x45x40 mm) in order to verify cutting forces at different radial depth values. When determining the material constants, there was only one radial depth of cut (45 mm). It was machined through face symmetrical milling.

4.4 Experiment design

To design the experiments, Taguchi planning was used for each radial depth of cut, thus for the values of 25, 35 and 45 mm, with the following cutting conditions:

- axial depth of cut: 1, 2 and 3 mm,
- feed per tooth: 0.09, 0.155 and 0.22 mm,
- cutting speed: 100, 200 and 300 m/min.

The proposed experiment plan is shown along with the results in Table 6.

4.5 Evaluation of experiments and verification of the proposed mathematical model

The mean values of the cutting force per engagement were evaluated using the measured force signals. As mentioned above, each experiment was measured twice and from these values, the mean value was determined. Furthermore, the values of cutting forces per engagement were calculated using the proposed mathematical model.

To compare the experimentally determined and calculated values of the cutting force, we used equation (30) which expresses the percentage deviation of both values (ΔF_c).

$$\Delta F_c = \frac{F_{c_{exp}} - F_{c_{mod}}}{F_{c_{exp}}} \cdot 100 \qquad (30)$$

Table 6 shows the percentage deviation between the experimentally determined and calculated values. Two mathematical models were used for the verification. The first mathematical model (Model 1) does not include the impact of the corner radius and the second mathematical model (Model 2) does not include the impact of the corner radius.

No.	Cutting conditions				Verification				
	a_e [mm]	a_p [mm]	f_t [mm]	v_c [m/min]	F_c [N] Experiment	Model 1	Model 2	ΔF_{c_Model1} [%]	ΔF_{c_Model2} [%]
1	25	1	0.09	100	331.3	265.5	326.7	19.9	1.4
2			0.155	200	391.5	328.5	406.7	16.1	-3.9
3			0.22	300	452.0	379.6	472.5	16.0	-4.5
4		2	0.09	200	477.6	469.0	527.8	1.8	-10.5
5			0.155	300	641.7	611.0	690.3	4.8	-7.6
6			0.22	100	1091.0	924.2	1047.9	15.3	3.9
7		3	0.09	300	660.0	654.3	710.6	0.9	-7.7
8			0.155	100	1184.7	1115.7	1215.3	5.8	-2.6
9			0.22	200	1314.2	1224.5	1337.5	6.8	-1.8
10	35	1	0.09	100	344.8	264.4	325.4	23.3	5.6
11			0.155	200	388.6	327.1	405.0	15.8	-4.2
12			0.22	300	473.6	378.0	470.6	20.2	0.6
13		2	0.09	200	500.1	467.1	525.6	6.6	-5.1
14			0.155	300	658.5	608.5	687.4	7.6	-4.4
15			0.22	100	1074.8	920.3	1043.5	14.4	2.9
16		3	0.09	300	674.6	651.6	707.7	3.4	-4.9
17			0.155	100	1346.0	1111.1	1210.3	17.5	10.1
18			0.22	200	1314.2	1219.4	1332.0	7.2	-1.4
19	45	1	0.09	100	354.2	262.9	323.5	25.8	8.7
20			0.155	200	430.4	325.3	402.7	24.4	6.4
21			0.22	300	462.9	375.8	467.9	18.8	-1.1
22		2	0.09	200	527.4	464.4	522.5	12.0	0.9
23			0.155	300	687.3	605.0	683.5	12.0	0.6
24			0.22	100	1270.3	915.0	1037.5	28.0	18.3
25		3	0.09	300	741.9	647.8	703.6	12.7	5.2
26			0.155	100	1299.5	1104.7	1203.3	15.0	7.4
27			0.22	200	1313.9	1212.4	1324.3	7.7	-0.8
Evaluation					Minimum deviation			0.9	-10.5
					Maximum deviation			28.0	18.3
					Mean deviation			15.1	2.5

Table 6. Experimentally determined and calculated cutting forces and their verification.

The mean value of the percentage deviation (ΔF_c) is 15.1% for the model without consideration of the rounded part of the cutting edge (Model 1) and 2.5% for the model that considers both the rounded and straight parts (Model 2).

The analysis of the two mathematical models also shows that when using Model 2, 59% of all experiments are in the deviation interval of -5 to 5%, unlike Model 1, where only 15% of all experiments are in this deviation interval. In the deviation interval from -10 to 10%, 89% of all experiments are in the interval when using Model 2 and only 37% of all experiments when using Model 1.

The analysis of the two models shows that the model considering the rounded as well as the straight part of the cutting edge is more accurate.

5 GENERALIZATION OF THE PROPOSED MODEL

5.1 Generalization of the mathematical model for cutting tools with a different rake angle

Of the geometrical characteristics of the cutting tool, the orthogonal rake angle (γ_o) is one of the factors that has a very significant effect on the specific cutting force. Its influence is associated with the primary plastic deformation of the cutting process. The more positive the rake angle is, the smaller the area of primary plastic deformation, and thus the specific cutting force is reduced; see Figure 9. [Madl 1989]

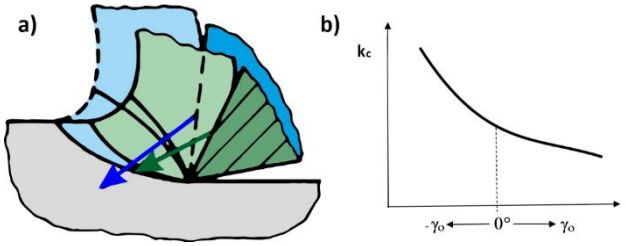

Figure 9. Dependence of rake angle on: a) the change of the area of primary plastic deformation, b) the specific cutting force [Madl 1989].

The material constants for calculating the specific cutting force are always determined when cutting by using a cutting tool with some value of the rake angle. To predict the cutting force,

however, we want to use a different cutting tool that has a rake angle that is often very different. If the rake angle of the cutting tool used for the experiments to get material constants is very different from the cutting tool for which we want to predict the cutting force, it should be expected that the calculation will be inaccurate. In the references [Degner 2015, Gazda 1993, Tschatsch 2009] we can find the correction factor of the rake angle, which recalculates the specific cutting force for a cutting tool with different rake angles; see equation (31).

$$K_{\gamma_o} = 1 - (0.01 \div 0.015) \cdot \Delta\gamma_o \quad (31)$$

The calculation of the correction factor of the rake angle is based on the rake angle of the cutting tool used in experiments in which the material constants were obtained, i.e. γ_{oo}, and the rake angle of the cutting tool for which the cutting force is predicted, i.e. γ_{oakt}. The parameter $\Delta\gamma_o$ is calculated as the difference of these two angles: $\Delta\gamma_o = \gamma_{oakt} - \gamma_{oo}$.

Equation (31) shows that if $\Delta\gamma_o$ is equal to +1°, which means that γ_{oakt} is 1° higher than γ_{oo}, the correction factor decreases by 1 to 1.5%. The higher the rake angle difference $\Delta\gamma_o$, the higher the decrease of the correction factor and thus the specific cutting force. If we want to predict the cutting force for a cutting tool where is $\Delta\gamma_o = \pm 10°$, the specific cutting force changes by $\mp(10 \div 15)\%$, which is a relatively big error. This is why this correction factor should be used.

Verification of rake angle impact on specific cutting force

The aim of this chapter is to verify the effect of the rake angle on the change of the specific cutting force, i.e. whether the equation for the correction factor of the rake angle for the recalculation of the specific cutting force stated above is valid.

Based on the reseach data of professor Madl, the co-author of this article, the correction factors of the rake angle are summarized in Table 7.

	Rake angle γ_o [°]				
	5	0	-5	-10	-15
K_{γ_o}[-]	0.85	0.90	0.95	1	1.06

Table 7. Correction factors of the rake angle obtained by face milling

These correction factors were obtained when milling steel with a tensile strength of 750 MPa. The rake angle of the cutting tool used to obtain the material constants in this case was -10°; therefore the correction factor for the rake angle -10 ° is 1.

Based on the data shown in Table 6, a dependence of the correction factor of the rake angle on the rake angle is made, see Figure 10.

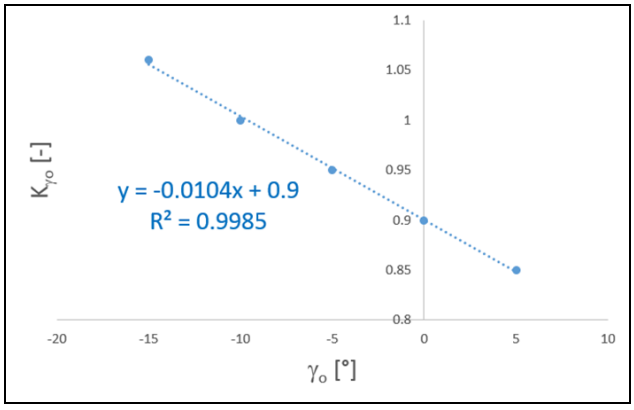

Figure 10. Dependence of the correction factor of the rake angle on the rake angle within for the steel with a tensile strength of 750 MPa

To get the correction factor equation, linear regression was used for the data. The obtained equation in Figure 10 shows the following impact of the rake angle on the specific cutting force: if $\Delta\gamma_o$ is equal to +1°, which means that γ_{oakt} is 1° higher than γ_{oo}, the correction factor decreases by 1%. Thus, equation (31) was confirmed, and based on the verification of the rake angle effect, we can use the correction factor of the rake angle as equation (32) shows.

$$K_{\gamma_o} = 1 - 0.01 \cdot \Delta\gamma_o \quad (32)$$

The specific cutting force with the rake angle effect is then given by equation (33).

$$k_c = k_{c_{1.1}} \cdot h_D^{-m_c} \left(\frac{v_c}{v_{c_{def}}} \right)^{-m_{v_c}} \cdot (1 - 0.01 \cdot \Delta\gamma_o) \quad (33)$$

5.2 *Generalization of the mathematical model for cutting tools with a different number of teeth*

In Chapter 2, a mathematical model for calculating the mean value of the cutting force per tooth was created. It is now necessary to generalize this model to calculate the mean value of the cutting force per revolution for a different number of teeth in engagement. This value can be used to calculate the mean value of cutting power, machine tool power and torque. The calculated value of the cutting power from the mean value of the cutting force per revolution is also important for calculating the energy consumption of the cutting process.

For the calculation of the mean value of the cutting force for Z teeth in engagement per revolution, the mean cutting force per tooth and number of teeth in contact (Z_e) are used; see equations (34) and (35) [Degner 2015, Tschatsch 2009].

$$F_{c_m} = Z_e \cdot F_{c_{m1z}} = \frac{1}{2\pi} \cdot Z \cdot \varphi_{eng} \cdot F_{c_{m1z}} \quad (34)$$

$$F_{c_m} = \frac{1}{2\pi} \cdot k_{c_{1.1}} \cdot \left(\frac{v_c}{v_{c_{def}}} \right)^{-m_{v_c}} b_D \cdot Z \cdot \int_{\varphi_{st}}^{\varphi_{end}} h_D(\varphi)^{1-m_c} \, d\varphi \quad (35)$$

6 EFFECT OF TOOL FLANK WEAR ON CUTTING FORCE

6.1 *Motivation and principle for refining the model*

According to the references [Degner 2015, Madl 1989, Tschatsch 2009, Vasilko 2007], the tool flank wear (VB) has a significant effect on the cutting force and thus the cutting power. The impact of tool flank wear is related to the change of the area of primary plastic deformation. The greater the tool flank wear (VB), the greater the cutting edge radius (ρ), thereby the area of primary plastic deformation increases, which causes a higher specific cutting force; see Figure 11.

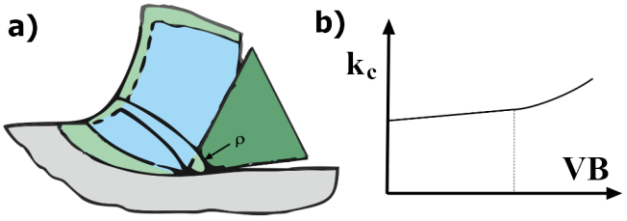

Figure 11. a) Area change of primary plastic deformation, b) Dependence of specific cutting force on tool flank wear [Madl 1989]

The effect of the tool flank wear (VB) on the cutting force is usually expressed by the tool flank wear correction factor (K_{VB}). The value of the correction factor for the specific tool flank wear value (VB) is certainly dependent on the specific workpiece material and cutting conditions. The following cutting conditions have the highest impact on tool flank wear:

cutting speed, feed per tooth and axial depth of cut. It is therefore clear that there is a different correction factor value for a specific tool flank wear value and different combination of values of the mentioned cutting conditions. To make the correction factor as precise as possible, we would have to conduct many experiments with different combinations of cutting conditions, which would be very time-consuming and quite expensive. However, It is possible to develop a simplified equation, which would express the correction factor only as a function of the tool flank wear by using one set of cutting conditions.

It should be mentioned that the material constants for calculating the specific cutting force (k_c) are, or should be, obtained by using a new cutting tool insert, therefore the tool flank wear correction factor for this case is 1 (K_{VB}=1). The greater the tool flank wear value, the higher the correction factor.

6.2 *Preparation of experiments*

The experiments were carried out at the Research Center of Manufacturing Technology, Czech Technical University in Prague, on a MCFV 5050LN three-axis milling center made by the company ZPS Tajmac, Czech Republic.

A 125B09R-W75SP12D cutting tool (D=125mm, κ_r=75°, λ_s=0°, γ_o=0°) with SPKN1203EDSR cutting tool inserts was used for these experiments. The cutting tool inserts were made of carbide and there were three types of PVD coatings. The specific composition of the coatings cannot be published to protect the client's intellectual property.

These experiments were performed on DIN C45 steel with a measured hardness of 200 ± 10 HB. The workpiece material dimensions were 400 x 102 mm (length x width).

The cutting conditions were set with respect to the requirements of the company for which the research was performed: v_c=240m/min, f_z=0.2mm, a_p=2mm, a_e=102mm.

6.3 *Measurement and evaluation methodology*

The aim of the experiments was to measure the tool flank wear (VB) of the SPKN1203EDSR cutting tool inserts in face milling of DIN C45 steel without the use of cutting fluid. For some experiments we also measured the current and voltage with an ammeter and we got the power. To obtain the mean values of the cutting power, the total power (P) and the idle power (P_0) had to be evaluated. The cutting power (P_c) is the difference between these two powers; see Figure 12.

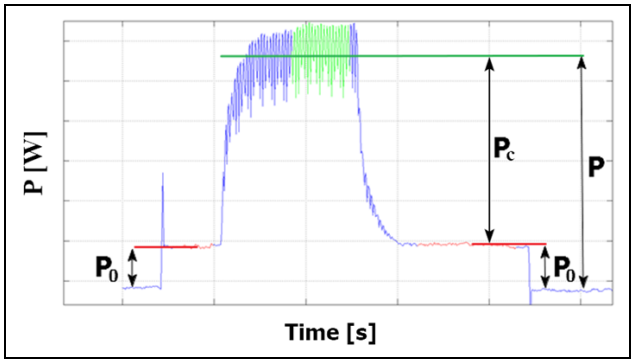

Figure 12. Evaluation of the cutting power from experimental data

6.4 *Evaluation of experiments and determination of equation for the tool flank wear correction factor*

Tool flank wear values were obtained for the cutting tool inserts with three types of coatings. Based on these values, the dependence of the tool flank wear on time was plotted; see Figure 13.

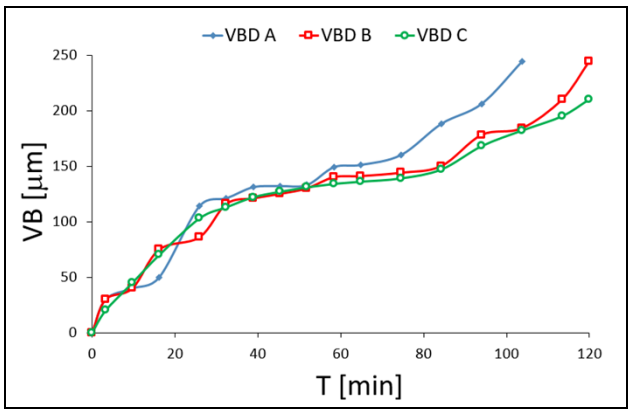

Figure 13. Dependence of the tool flank wear on time for the three types of cutting tool inserts (A, B, C)

As already mentioned, for some tool flank wear values, powers were measured, from which the cutting power was evaluated. Table 8 summarizes the values of cutting power (P_c), tool flank wear (VB) and time (T) for all three cutting tool inserts.

Cutting tool insert	Evaluated values from experimental data			Calculated values	
	P_c [W]	T [min]	VB [µm]	P_c [%]	K_{VB} [-]
A	1298	0.0	0	100	1.000
	1452	45.4	132	112	1.119
	1597	84.3	188	123	1.230
		103.7	244		
B	1313	0.0	0	100	1.000
	1441	45.4	125	110	1.097
	1527	84.3	150	116	1.163
	1683	119.9	244	128	1.281
C	1316	0.0	0	100	1.000
	1469	45.4	127	112	1.116
	1548	84.3	147	118	1.176
	1670	119.9	210	127	1.268

Table 8. Evaluated values from experimental data (cutting power [W] and tool flank wear in specific time) and calculated values (cutting power [%] and correction factor of the tool flank wear

Figure 14 shows the dependence of the correction factor and cutting power on the tool flank wear.

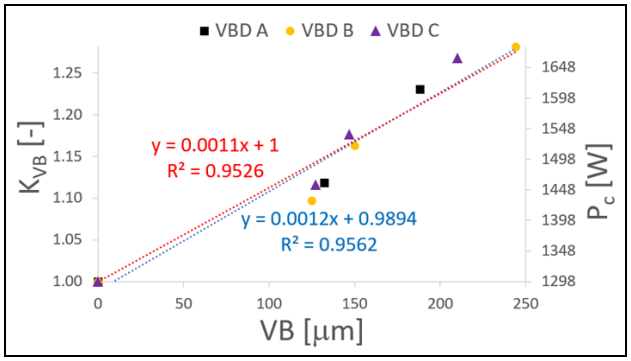

Figure 14. Dependence of the correction factor (KVB) and cutting power (P_c) on the tool flank wear (VB)

As seen in Figure 14, a linear regression was applied to the measured values. The dependence of the correction factor on the tool flank wear is expressed by equation (36).

$$K_{VB} = 0.0011 \cdot VB + 1 \quad (36)$$

The value of the correction factor with the zero value of the tool flank wear is 1. The dependence of the correction factor increases gradually from 1 to 1.27. The cutting power increases by 27% for a tool flank wear of 244 µm.

The specific cutting force equation is then improved by implementing the tool flank wear correction factor; see equation (37), which also shows the correction factor of the rake angle.

$$k_c = k_{c_{1.1}} \cdot h_D^{-m_c} \left(\frac{v_c}{v_{c_{def}}} \right)^{-m_{v_c}} \cdot K_{\gamma_o} \cdot K_{VB} \quad (37)$$

Based on equation (35), the dependence of the specific cutting force on feed per tooth for three values of tool flank wear was obtained; see Figure 15. In this case, the value of the parameter $\Delta\gamma_o$ is 0°.

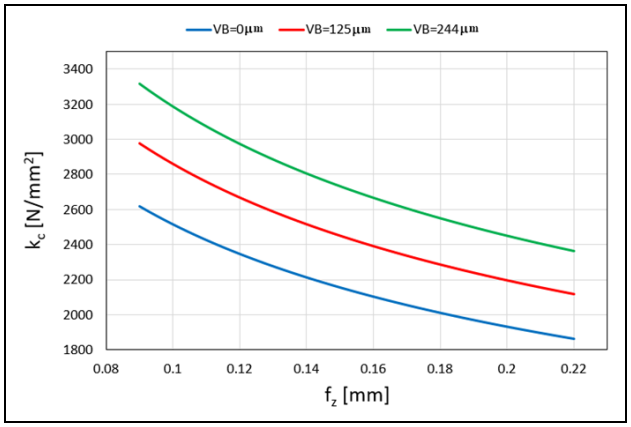

Figure 15. Dependence of the specific cutting force (k_c) on feed per tooth (f_z) for three values of tool flank wear (VB)

7 CONCLUSIONS

The main aim of this article was to propose a mathematical model for cutting force extended by the effect of the tool wear for milling by milling heads.

The first task was to create a mathematical model for the cutting force. We chose to use a method based on the specific cutting force and cutting area. The mathematical model, in comparison with other models, was refined by more accurate calculation of the specific cutting force and cutting area. The calculation of the specific cutting force was refined by considering the influence of the cutting speed as well as by more precise calculation of the undeformed chip thickness. The calculation of the cutting area was refined by more accurate calculation of the chip width as well as the undeformed chip thickness. The chip width and undeformed chip thickness was made more precise by considering the straight as well as the rounded part of the cutting edge.

The proposed mathematical model of the specific cutting force contains three material constants that had to be determined. The material constant $k_{c1.1}$ is a specific cutting force per area of 1 mm² and cutting speed v_{cdef}. The constant m_c determines the effect of the undeformed chip thickness on the specific cutting force. The material constant m_{vc} determines the influence of the cutting speed on the specific cutting force. To obtain the material constants, a measurement methodology was proposed such that only the straight part of the cutting edge acts when cutting a workpiece material. For this purpose, a sample with a fixture were designed. The material constants were obtained for the workpiece material made of DIN C45 steel. The value of the determination index (R^2) of the mathematical model for the specific cutting force was 94.88% and the value of the adjusted determination index (R^2 Adj) was 94.19%.

After obtaining the material constants, it was necessary to verify the mathematical model. In order to verify the calculated values of cutting forces, the percentage deviation of calculated and cutting force values found through the experiments was calculated. The mean value of percentage deviation was 15.1% for the model without considering the rounded part of the cutting edge (Model 1) and 2.5% for the model that considers the rounded and straight parts of the cutting edge (Model 2). The analysis of both mathematical models also shows that when using Model 2, 59% of all experiments are in the deviation interval from -5 to 5%, unlike Model 1, where only 15% of all experiments are in this deviation interval. When using Model 2, 89% of all experiments are in the deviation interval from -10 to 10%, and only 37% of all experiments when using Model 1. The analysis of both models shows that the model that considers the rounded as well as the straight part of the cutting edge is more accurate.

The next task was to generalize the proposed mathematical model by considering the orthogonal rake angle which has quite a significant impact on the specific cutting force. In the references [Degner 2015, Gazda 1993, Tschatsch 2009] we can find the correction factor of the rake angle, which recalculates the specific cutting force for a cutting tool with different rake angles. The correction factor equation was verified by experimental data obtained from milling a steel with a tensile strength of 750 MPa. After the verification, the equation for the correction factor of the rake angle was obtained and implemented into the specific cutting force equation.

The next task was to refine the proposed mathematical model by considering the tool wear effect. For this task, cutting tool inserts made of carbide with three types of PVD coatings were used. We decided to measure the tool flank wear as well as cutting power. From the measured tool flank wear and cutting power values, the dependence of the correction factor on the tool flank wear was determined and a correction factor equation was obtained. The value of the correction factor with the zero value of the tool flank wear is 1. The correction factor increases gradually from 1 to 1.27. The cutting power increases by 27% for tool flank wear of 244 μm.

ACKNOWLEDGMENTS

This paper was supported by a grant from the Technology Agency of the Czech Republic.

LIST OF SYMBOLS USED IN THIS ARTICLE

$\alpha(\varphi)$	rad	Angle between the actual values of the active force and the force in the Y-axis of the dynamometer coordinate system
φ	rad	Actual value of the engagement angle
φ_{end}	rad	Ending engagement angle
φ_{eng}	rad	Engagement angle
φ_{st}	rad	Starting engagement angle
φ_z	rad	Number between teeth
θ	rad	Actual angle of acting the rounded part of the cutting edge
θ_{end}	rad	Ending angle of acting the rounded part of the cutting edge
θ_{st}	rad	Starting angle of acting the rounded part of the cutting edge
$A_D(\varphi)$	mm²	Actual value of the cutting area
$A_{D1}(\varphi)$	mm²	Actual value of the cutting area of the straight part of the cutting tool edge
$A_{D2}(\varphi)$	mm²	Actual value of the cutting area of the rounded part of the cutting tool edge
a_p	mm	Depth of cut
b_D	mm	Chip width
b_{D1}	mm	Chip width of the straight part of the cutting tool edge
b_{D2}	mm	Chip width of the rounded part of the cutting tool edge
db_{D2}	mm	Element of the chip width of the rounded part of the cutting tool edge
$F_a(\varphi)$	N	Actual value of the active force

$F_c(\varphi)$	N	Actual value of the cutting force
$F_{c1z}(\varphi_i(\varphi))$	N	Actual value of the cutting force per tooth for the i-th tooth
F_{cm1z}	N	Mean value of the cutting force per tooth
$F_x(\varphi)$	N	Actual value of the force in the X-axis of the dynamometer coordinate system
$F_y(\varphi)$	N	Actual value of the force in the Y-axis of the dynamometer coordinate system
f_z	mm	Feed per tooth
h_D	mm	Undeformed chip thickness
$h_D(\varphi_i(\varphi))$	mm	Actual value of the undeformed chip thickness for the i-th tooth
$h_{D1}(\varphi)$	mm	Actual value of the undeformed chip thickness of the straight part of the cutting tool edge
$h_{D2}(\varphi,\theta)$	mm	Actual value of the undeformed chip thickness of the rounded part of the cutting tool edge
k_c	N/mm^2	Specific cutting force
$k_c(\varphi_i(\varphi))$	N/mm^2	Actual value of the specific cutting force for the i-th tooth
$k_{c1.1}$	N/mm^2	Specific cutting force per 1 mm^2 (h=b=1mm)
K_{VB}	-	Correction factor of the tool flank wear
m_c	-	Empirical constant (impact of undeformed chip thickness on the specific cutting force)
m_{vc}	-	Empirical constant (impact of cutting speed on the specific cutting force)
P_c	W	Cutting power
R	mm	Radius in the proposed mathematical model
r_ε	mm	Corner radius
s	N	Standard deviation
T	min	Time of reaching the tool flank wear
VB	μm	Tool flank wear
v_c	m/min	Cutting speed
v_{cdef}	m/min	Cutting speed which was used to obtain the material constants
Z	-	Number of teeth of the selected cutting tool

REFERENCES

[Aksu 2016] Aksu, B. and Celebi, C. An experimental investigation of oblique cutting mechanics. Machining Science and Technology. 2016. ISSN 1532-2483.

[Altintas 2012] Altintas, Y. Manufacturing Automation: Metal Cutting Mechanics, Machine Tool Vibrations and CNC Design. New York: Cambridge University Press, 2012. ISBN 978-0-521-17247-9.

[Constantin 2013] Constantin, C. and Constantin, G. Empirical model of the cutting forces in milling. Proceedings in Manufacturing Systems, 2013. ISSN 2067-9238.

[Degner 2015] Degner, W. and Lutze H. Spanende Formung: Theorie, Berechnung, Richtwerte. Munchen: Carl Hanser Verlag GmbH & Co. KG, 2015. ISBN 978-3-446-44544-4.

[Dobrzanski 2005] Dobrzanski, L. A. and Kowalski, M. Methodology of the mechanical properties prediction for the metallurgical products from the engineering steels using the Artificial Intelligence methods. Journal of Materials Processing Technology, 2005. ISSN: 0924-0136.

[Horvath 2017] Horvath, R. and Lukacs, J. Application of a Force Model Adapted for the Precise Turning of Various Metallic Materials. Strojniski vestnik - Journal of Mechanical Engineering, 2017. ISSN 00392480.

[Gazda 1993] Gazda, J. Theory of cutting: Forces in cutting. Liberec: VSST Liberec, 1993. ISBN 80-7083-110-3.

[Irgolic 2013] Irgolic, F. and Cus, M. Prediction of cutting forces with neural network by milling functionally graded material, Faculty of mechanical engineering, University of Maribor, Slovenia: 24th DAAAM International symposium on intelligent manufacturing and automation, 2013.

[Katsuhiro 2005] Katsuhiro, M. and Obikawa, T. Metal Machining – Theory and Applications. Leeds, England: Elsevier, 2000. ISBN 978-0-08-052402-3.

[Kolar 2016] Kolar, P. Electronic textbook of mathematical methods of physics. Faculty of Mathematics and Physics, Charles University, Department of Physics Education, 2016. Available: https://kdf.mff.cuni.cz/vyuka/matematicke_metody/Ucebnice_2.pdf.

[Kopacek 2004] Kopacek, J. Mathematical analysis not only for physicists (I). Faculty of Mathematics and Physics, Charles University in Prague, 2004. ISBN 80-86732-25-8.

[Kovalcik 2014] Kovalcik, J. and Zeman, P. Principles of Cutting Process Modelling and New Algorithm Proposal. Manufacturing Technology, December 2014, Vol. 14, No. 4. ISSN 1213-2489.

[Madl 1989] Madl, J. Theory of cutting. Prague: CVUT in Prague, Faculty of Mechanical Engineering, 1989.

[Mavi 2016] Mavi, A. and Ozden, S. Prediction and experimental study on cutting forces of stepped austempering grey cast iron using artificial neural network, Volume-2, Issue-2: International Journal of Mechanical and Production Engineering, 2016.

[Roud 2011] Roud, P. and Sklenicka, J. Using FEM in prediction of chip shape. Advances in manufacturing science and technology, 2011. ISSN 1895-9881.

[Starchurski 2012] Starchurski, W. and Midera, S. Determination of Mathematical Formula for the cutting force during the turning of C45 steel. Mechanics and Mechanical Engineering, Technical University of Lodz. 2012.

[Tschatsch 2009] Tschatsch, H. Applied Machining Technology. Berlin, Germany: Springer, 2009. ISBN 978-3-642-01006-4.

[Vasilko 2007] Vasilko, K. Analytical theory of cutting. Kosice, Slovakia: Faculty of Production Technologies, 2007. ISBN 8080737597.

[Vavruska 2018] Vavruska, P. and Zeman, P. Reducing Machining Time by Pre-Process Control of Spindle Speed and Feed-Rate in Milling Strategies. Procedia CIRP, Vol. 77, 2018. ISSN 2212-8271

[Velchev 2011] Velchev, S. and Kolev, I. Empirical mathematical models of the dependence of the specific cutting force on thickness of cut in turning. Annals of Faculty Engineering Hunedoara - International Journal of Engineering. 2011. ISSN 1584-2673.

[Zeman 2005] Zeman, P. and Madl, J. The Effect of High Cutting Speed on the Chip Formation Process. 8th CIRP International Workshop on Modelling of Machining Operations, University of Warwick. ISBN 3-937524-24-X.

[Zhang 2018] Zhang, X. and Zhou, H. A novel milling force model based on the influence of tool geometric parameters in end milling. Advances in Mechanical Engineering, 2018. ISSN 16878140.

CONTACTS:

Ing. Jaroslav Kovalcik
Department of Production Machines and Equipment, Faculty of Mechanical Engineering, Czech Technical University in Prague
Horska 3, 128 00 Praha 2, Czech Republic
+420 221 990 976, j.kovalcik@rcmt.cvut.cz, www.rcmt.cvut.cz